Diagnosis of magnetic structures and intermittency in space-plasma turbulence using the technique of surrogate data

F. Sahraoui*
Goddard Space Flight Center, NASA, Greenbelt, Maryland 20771, USA
and Centre d'Etude des Environnements Terrestre et Planétaires, CETP/CNRS–UVSQ, 10/12 av. de l'Europe, 78140, Vélizy, France
(Received 14 March 2008; revised manuscript received 2 June 2008; published 5 August 2008)

Intermittency is usually identified in turbulent flows as non-Gaussian tails of the probability density functions (PDFs) of the turbulent field derivatives. Here we investigate the role of phase coherence among the Fourier modes in creating intermittency in magnetized space plasmas using the technique of surrogate data. We apply the technique to two examples: (i) synthetic data and (ii) magnetic field fluctuations recorded in the terrestrial magnetosheath by the Cluster spacecraft. We use a set of four series of data, one observed and three surrogate, and their PDFs and moments ($q \leqslant 4$) as discriminating statistics. We show that the technique allows for detecting coherent structures and estimating their scales. We show furthermore that the phases, but not the amplitudes, create the non-Gaussian tails of the PDFs. We show also that the surrogate data used cannot account for asymmetries of the PDFs of the observed data. This enables us to confirm a scenario of turbulent cascade of mirror structures proposed in previous publications, by showing the existence of an approximately constant energy flux in the inertial range.

DOI: 10.1103/PhysRevE.78.026402 PACS number(s): 52.35.Ra, 94.05.Lk, 94.30.cj, 94.30.cq

I. INTRODUCTION

Turbulence in magnetized space plasmas has been studied extensively over the past several years to understand its role in fundamental processes such as mass transport, energy dissipation, and magnetic reconnection [1–6]. In the solar wind and in the terrestrial magnetosphere, the Cluster space craft data have made it possible to reveal new properties of magnetic turbulence, in particular its three-dimensional spatial spectra [7–11]. However, these energy spectra (where phases are missed) cannot fully characterize nonlinear interactions of plasma waves. The same holds for related quantities such as the autocorrelation functions or the wavelet coefficients [12]. For instance, they cannot account for the strength of nonlinearities (weak or strong) important in theoretical modeling of turbulence, or prove the presence of energy cascades. Very often, observations of power law spectra are promptly interpreted as signatures of turbulent energy cascades. Yet, as we will show below, power law spectra can also be created by single coherent structures with which no energy cascade or inertial range can be associated.

Here we propose to go further by analyzing the Fourier phases of turbulence and study their role in creating intermittency as well as in the energy cascade. From the theoretical point of view, phases are known to be the vehicle for nonlinear interactions and energy transfers between different eigenmodes and scales of any dynamical system. One would therefore investigate the structure of the phases in order to detect nonlinearities [13,14]. Yet, in space-plasma turbulence very limited work exists on the use of phases as potential tracers of nonlinearities. The reason why the phases are seldom used is probably because they usually appear to be completely random (due to their dependence on an arbitrary time origin and to 2π ambiguity) [12,15–17].

Making it possible to study phase coherence properly is an important issue regarding theories of weak turbulence. Indeed, these theories generally use the random phase approximation (RPA) to derive power law spectra of turbulence [18–20]. While the predicted spectra are often compared to various astrophysical observations, to the best of our knowledge, no test has been proposed to check within data the validity of the RPA and thus to determine the applicability limit of weak turbulence models when used to describe space-plasma turbulence [21,22].

II. SURROGATE DATA TECHNIQUE

The technique of *surrogate data*, named also the *null hypotheses* method, is widely used in the dynamical systems community [13,14,23]. We first review its major principles before showing the specific use and adaptations we have introduced in the present work. Given an observed time series $B_O(t)$ we formulate null hypotheses against which $B_O(t)$ is tested; here that $B_O(t)$ *is coherent* or $B_O(t)$ *is random*. Then we build a surrogate signal that satisfies each hypothesis: $B_R(t)$ for *random* and $B_C(t)$ for *coherent*. We impose, however, the requirement that $B_R(t)$ and $B_C(t)$ share the autocorrelation function of $B_O(t)$ (or, equivalently, its Fourier amplitudes). Then, a set of discriminating statistics is computed for both the original and the surrogate data. If the value obtained for $B_O(t)$ is significantly different from that of a surrogate signal then the corresponding hypothesis is rejected.

In practice, we perform a windowed Fourier transform of the signal $B_O(t)$ which yields the amplitude spectrum $|B(f)|$ and the phases $\Phi_O(f)$. We create two sets of phases: coherent phases (i.e., with a linear dependence on the frequency) $\Phi_C(f)$ and randomly distributed phases $\Phi_R(f)$. Then, using an inverse Fourier transform $\mathcal{F}^{-1}$ we reconstruct two surrogate signals sharing the same power spectrum $|B(f)|$, but having different phases: $B_C(t)=\mathcal{F}^{-1}[|B(f)|e^{-i\Phi_C(f)}]$ and

*fsahraoui@pop600.gsfc.nasa.gov; fouad.sahraoui@cetp.ipsl.fr

 ©2008 The American Physical Society

$B_R(t)=\mathcal{F}^{-1}[|B(f)|e^{-i\Phi_R(f)}]$. In order for the inverse Fourier transform to be real (no imaginary part) we impose the symmetrization of the phases $\Phi(-f)=-\Phi(f)$. The window function is introduced here to minimize the boundary effect when determining the Fourier coefficients. The window chosen is a *cosine cube-tapered rectangle* function: a rectangle function over 80% of the studied time interval T, which tapers off as a $\cos^3$ function over 10% at each end of T. This is shown to be the most appropriate window for the purpose of this work.

In addition to the three previous data sets we use a fourth one, $B_{\mathrm{PDF}}(t)$, constructed by a random shuffling of $B_O(t)$. This implies that the two signals share the same probability density function (PDF) of the data, but the Fourier spectrum is no longer conserved. Random shuffling ensures that any existing correlation among the amplitudes and the phases in the data is destroyed.

Because the purpose here is to relate phase coherence to intermittency we use the PDFs of the increments and their moments, or, equivalently, their structure functions (SFs) $S(q,\tau)$ as discriminating statistics between the different hypotheses:

$$S_i(q,\tau)=\langle|\delta B_i(t,\tau)|^q\rangle_t=\langle|B_i(t+\tau)-B_i(t)|^q\rangle_t.$$

Here $i\in[O,R,C,\mathrm{PDF}]$, τ is the time lag, and the angular brackets denote a time average. Use of the moments of the PDFs of increments is very common in intermittency studies. However, as we will show below, using in addition appropriate surrogate data as "experimental boundary conditions" allows for additional insights and can help avoid pitfalls and misinterpretations of the data.

To quantify the differences between the SFs of the different signals *for each order q* we introduce a general index of coherence $C_\Phi(q,\tau)$ that measures the "relative distances" between the curves $S_O(q,\tau)$, $S_R(q,\tau)$, and $S_C(q,\tau)$:

$$C_\Phi(q,\tau)=\left(\frac{|S_O(q,\tau)-S_R(q,\tau)|}{|S_O(q,\tau)-S_R(q,\tau)|+|S_O(q,\tau)-S_C(q,\tau)|}\right)^{1/q}.$$

$C_\Phi(q,\tau)=1(0)$ for a coherent (random) signal. The power $1/q$ is introduced to give equal weight to each order of the SF when comparing the results given by each order of $C_\Phi(q,\tau)$. $S_{\mathrm{PDF}}(q,\tau)$ cannot be used in this estimation of coherence as $B_{\mathrm{PDF}}(t)$ does not conserve the same power spectrum $|B(f)|$. However, it will be introduced below for comparisons between the PDFs of the different data sets. For $q=1$ this coefficient is comparable to the one used in [15,17]. We notice here that because the three data sets have the same variance (or power spectrum) the equality $S_O(2,\tau)=S_R(2,\tau)=S_C(2,\tau)$ is theoretically satisfied [i.e., $S(2,\tau)$ is not phase dependent] [24]. Therefore, $S_i(2,\tau)$ cannot discriminate between different natures of phases. However, any departure from the equality above can be attributed to statistical errors in estimating the SF (finite length of time series, nonstationarity, etc.). We propose therefore to use $S_i(2,\tau)$ as a measure of the accuracy in the determination of the SF. We define the quality factor $Q(\tau)$ as the variance of the different realizations of $S(2,\tau)$:

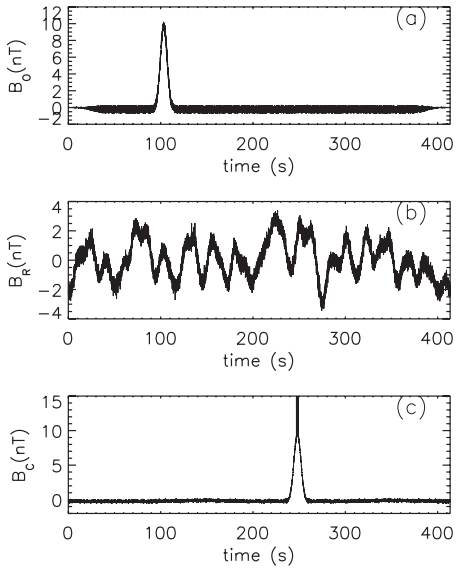

FIG. 1. (a) Original signal $B_O(t)$; (b) and (c) two surrogate data sets $B_R(t)$ and $B_C(t)$ with random and coherent phases.

$$Q(\tau)=\frac{\sqrt{\langle[S_O(2,\tau)-S_i(2,\tau)]^2\rangle_{i=R,C}}}{S_O(2,\tau)}.$$

$Q(\tau)\sim 0$ (or ~ 1) reflects a minimum (or maximum) discrepancy between the $S(2,\tau)$ of the three data sets. Under the hypothesis that the errors in calculating $S(2,\tau)$ occur for other orders of the SF, $Q(\tau)$ provides a simple way to quantify noise at large scales due to the finite length of the time series, providing thus an estimation of the largest scale $\tau_{\max}$ for which one can calculate the SF. If we consider reliable only scales for which $Q(\tau)\leqslant 10\%$, then we generally obtain in the present study $\tau_{\max}\sim T/4$.

III. PHASE COHERENCE AND INTERMITTENCY

Let us start first with a simple example to illustrate how the technique works. Consider a signal composed of a coherent structure ($\sim e^{-t^2}$) and a random noise of 10% of the amplitude of the structure [Fig. 1(a)]. Two surrogate data sets are generated as described above [Figs. 1(b) and 1(c)]. The coherent signal $B_C(t)$ is unsurprisingly akin to $B_O(t)$, since $B_O(t)$ contains a coherent structure by construction. However, the amplitude of the structure in $B_C(t)$ is higher because the random noise is suppressed while the power spectrum is conserved [$|B_O(f)|=|B_C(f)|$].

Figure 2 shows the four first-order SFs of $B_O(t)$, $B_C(t)$, and $B_R(t)$. As we can observe, the curves $S_O(q,\tau)$ have a random behavior at small scales and depart from the random curves $S_R(q,\tau)$ toward the curves $S_C(q,\tau)$ at scales close to the scale of the structure [Fig. 2(a)]. This can be explained by the dominance of random fluctuations at small scales whereas a coherent structure is detected at larger ones. This is confirmed by the coherence index, which vanishes at small scales and reaches its maximum value $C_\Phi(q,\tau)\sim 0.9$ for $\tau\sim 20$ s (Fig. 3). It is worth noticing that higher-orders SFs show the same level of coherence. This suggests that the

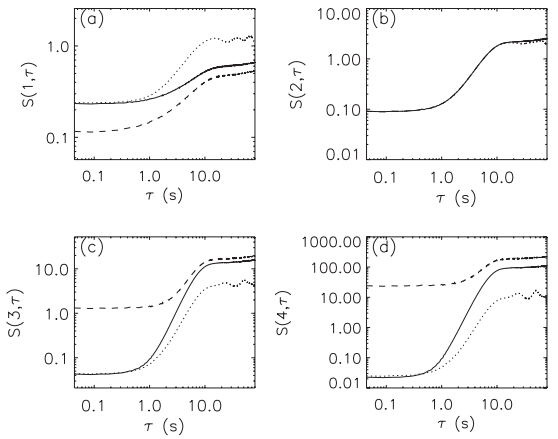

FIG. 2. SFs of observed data $B_O(t)$ (solid line) and surrogate data: $B_R(t)$ (dotted line), $B_C(t)$ (dashed line).

first-order SFs of the observed and the surrogate data would be sufficient to characterize phase coherence. We will return to this issue further below. Figure 3 shows also how accurately the three data sets reproduce the power spectrum or the variance shown in Fig. 2(b). The discrepancies are found to be less than 10% in the studied interval of scales. This example shows the capability of the method to detect both random fluctuations and coherent structures and determine their scales. Other tests (not shown here) have been performed and have confirmed the robustness of the method.

Consider now the magnetic field data measured by the Cluster satellite on February 18th, 2002 about 5:10 UT [Fig. 4(a)]. The data were recorded in the magnetosheath (part of the solar wind that is downstream of the terrestrial bow shock). These data have been studied in previous work and shown to be dominated by mirror modes [10,25]. Mirror modes are compressible, nonpropagating modes that grow in a hot plasma because of an ion temperature anisotropy. In that work, based only on the study of the power spectra and the derived dispersion properties, a $k^{-8/3}$ power spectrum was found [10]. A scenario of turbulent cascade of the mirror modes was then suggested to explain the observed power law. However, this scenario has not been proved. Moreover, the question whether the observed mirrors are randomlike modes or coherentlike structures could not have been answered using only the power spectra. Here we go further in answering these questions, which are important regarding theoretical modeling of mirror modes [26].

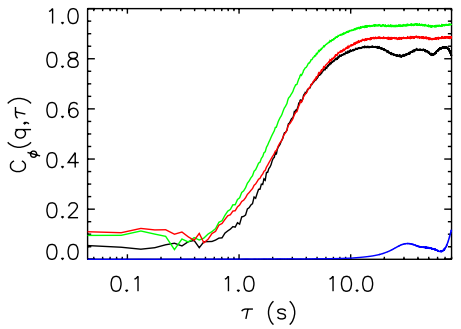

FIG. 3. (Color online) Coherence index $C_\Phi(q,\tau)$ estimated from different orders of the SF: $C_\Phi(1,\tau)$ (black), $C_\Phi(3,\tau)$ (green), and $C_\Phi(4,\tau)$ (red). The blue curve is the quality factor $Q(\tau)$ of estimation of the SF.

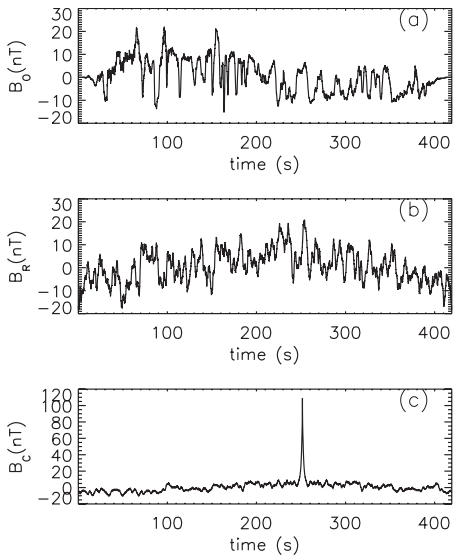

FIG. 4. (a) Magnetic field fluctuations measured by the Cluster spacecraft in the terrestrial magnetosheath, in the direction parallel to the local magnetic field. (b), (c) Two surrogate data sets $B_R(t)$ and $B_C(t)$ with random and coherent phases. The three signals, however, share the same power spectrum.

The two surrogate data sets $B_R(t)$ and $B_C(t)$ are presented in Figs. 4(b) and 4(c). The SFs of the four data sets are shown in Figs. 5(a)–5(d) with approximate power laws. First, notice that $S_O(q,\tau)$ show two regions with different scaling laws: a flat zone with a slope $n\sim 0$ at large scales ($\tau \geqslant 8$ s) and a clear power law at smaller scales with a slope $n \sim 1.5$. For $S_O(2,\tau)$ this results in power law scaling of the Fourier amplitudes $B^2(f)\sim f^{-\alpha}$ with two different slopes, respectively $\alpha\sim 1$ and $\alpha\sim 2.5$, since $\alpha=n+1$ [24]. The spectrum f^{-1} reflects the absence of correlations at large scale (i.e., the increments of the fluctuations are Gaussian). This is confirmed by the SFs of the signal $B_{\mathrm{PDF}}(t)$ which fit well those of the observed data $B_O(t)$ at large scales (Fig. 5).

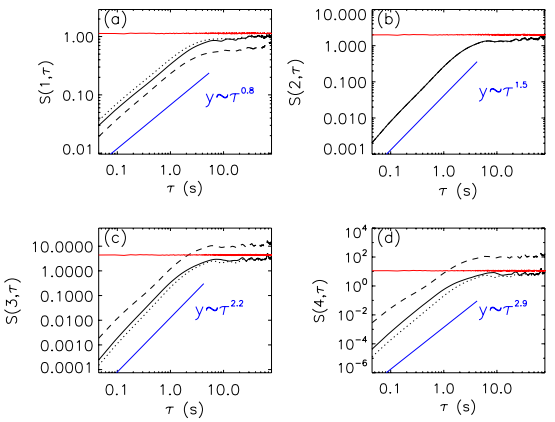

FIG. 5. (Color online) The SF of observed data set $B_O(t)$ (solid line) and the surrogate data sets $B_R(t)$ (dotted line), $B_C(t)$ (dashed line), and $B_{\mathrm{PDF}}(t)$ (red line). Power laws are shown for comparisons (blue lines).

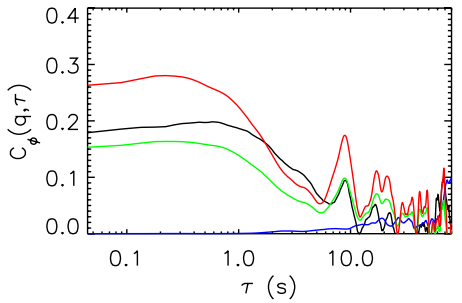

FIG. 6. (Color online) Coherence index estimated from different orders of the SF: $C_\Phi(1,\tau)$ (black), $C_\Phi(3,\tau)$ (green), $C_\Phi(4,\tau)$ (red). The blue curve is the quality factor $Q(\tau)$.

For scales below 8 s we observe, however, a clear discrepancy between $S_{\mathrm{PDF}}(q,\tau)$ and the SFs of the other signals, indicating that correlations in the amplitudes form [as $B_O(t)$, $B_C(t)$, and $B_R(t)$ have power law spectra, but not $B_{\mathrm{PDF}}(t)$]. Furthermore, for the same scales $S_O(q,\tau)$ depart slightly from $S_R(q,\tau)$ and approach $S_C(q,\tau)$, which indicates that phase coherence forms. This can be seen on Fig. 6 where the coherence indices $C_\Phi(q,\tau)$ almost vanish at large scale (although some noise is observed), and then increase significantly for $\tau\sim 8$ s and smaller scales, before they saturate for $\tau<0.5$ s. Both the change of the scaling and the appearance of coherence below $\tau\sim 8$ s suggest that nonlinear effects are at work and correlations among the fluctuations form. As in the previous example, we can see that all orders of the SF give very similar results, although $C_\Phi(4,\tau)$ provides a slightly higher level of coherence. Note that the surrogate data reproduce the power spectrum with an accuracy better than 95% for the studied scales. Figure 3 (where coherence is detected at large scales) and Fig. 6 (where coherence is detected at small ones) prove the capability of the method to detect coherent structures without prior assumptions on the range of scales involved. We notice that the interpretation the of time lags τ as spatial scales is based upon the Taylor hypothesis $l\sim v\tau$ (v is the plasma flow velocity), which is valid in this particular case of mirror structures [10]).

It is worth recalling here that it has been shown in [10] that the maximum of the mirror instability is observed at the scale $\tau\sim 8$ s and an inertial range forms down to the scale $\tau\sim 0.5$ s. The corresponding inertial range in wave number was shown to span from $k_v\rho\sim 0.3$ ($L\sim 1800$ km) to $k_v\rho\sim 3.5$ ($l\sim 150$ km), where k_v is the wave number along the flow direction and $\rho\sim 75$ km is the proton gyroradius. This agrees remarkably well with the results obtained above on phase coherence of the mirror modes. Also, the scaling in wave number $k^{-8/3}$ obtained by the k-filtering technique is very close to the scaling we can derive here from Fig. 5(b): $S(2,\tau)\sim\tau^{1.5}\sim l^{1.5}$ yielding $B(k)\sim k^{-2.5}$.

To relate these observations to intermittency we compare the PDFs of the increments of the four data sets calculated for different time lags τ. Here, we show the results for two scales, $\tau\sim 1$ and ~ 45 s, which have been chosen to fall into the inertial range (where coherence is increasing) and the flat zone (where coherence is absent). As we can see, $B_O(t)$ has almost a Gaussian distribution at large scale and departs from Gaussianity at small scales where clear tails appear

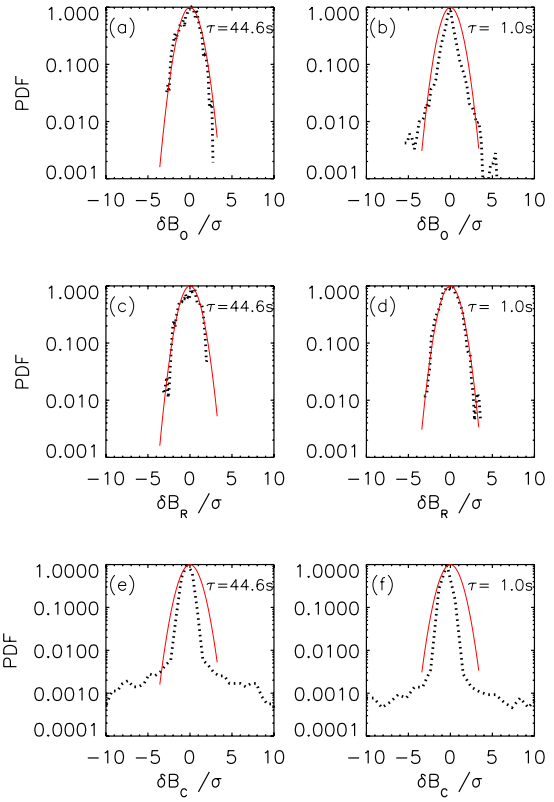

FIG. 7. (Color online) PDFs of the derivatives of $B_O(t)$ (a), (b), $B_R(t)$ (c), (d), $B_C(t)$ (e), (f) and $B_{\mathrm{PDF}}(t)$ used as a Gaussian fit (red curve). All PDFs are normalized to their respective variances. Two time scales are chosen: $\tau\sim 45$ (left panel) and ~ 1 s (right panel).

[Figs. 7(a) and 7(b)]. On the other hand, the PDFs of $B_R(t)$ are Gaussian at both large and small scales [Figs. 7(c) and 7(d)], whereas the PDFs of $B_C(t)$ exhibit clear non-Gaussian tails at the same scales [Figs. 7(e) and 7(f)]. These observations prove that the phases are responsible for creating intermittency while the amplitudes have no significant role.

This result can be confirmed by a direct measure of intermittency given by the flatness $F(\tau)=S(4,\tau)/S(2,\tau)^2$ [24]. For a Gaussian process $F(\tau)=3$. The flatness of the four signals are presented in (Fig. 8). The signal $B_R(t)$ is shown to have the flatness of a Gaussian process, whereas that of $B_O(t)$ departs clearly from this value at the scale $\tau\sim 8$ s and below in total agreement with the phase coherence estimation given

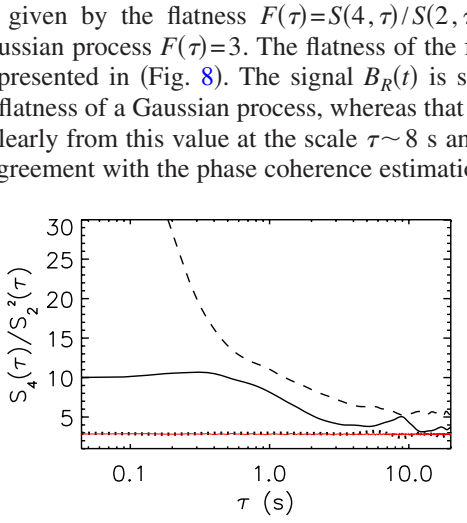

FIG. 8. (Color online) Flatness of $B_O(t)$ (solid line), $B_R(t)$ (dotted line), $B_C(t)$ (dashed line), and $B_{\mathrm{PDF}}(t)$ (red line). The flatness of $B_C(t)$ is, however, normalized to 10 to fit with the plot range.

above. $B_C(t)$ in turn shows a high level of intermittency with an approximately exponential increase at small scales, also in agreement with the strong non-Gaussian tails of its PDFs shown above. This gives direct evidence that phase coherence is the source of intermittency. One can note in particular the similarity of the curve of the flatness of $B_O(t)$ (Fig. 8) and the curves of the coherence level (Fig. 6).

IV. PHASE COHERENCE AND ENERGY CASCADE

The question now is whether the relatively moderate level of coherence $C_\Phi(q,\tau)\sim 0.3$ is crucial for the physics of the mirror structures observed here. Or, equivalently, whether the signals $B_O(t)$, $B_R(t)$, and $B_C(t)$ involve an energy cascade, as each of them has a power law spectrum, the two latter showing furthermore an increasing intermittency at small scales. Answering these questions requires a look at the asymmetries of the PDFs, whose estimation can be obtained from the third-order SFs for *signed* increments. It is indeed well known that the skewness provides information on nonlinearities and energy cascades [24]. For instance, in hydrodynamic turbulence the so-called Kolmogorov four-fifths law $S(3,l)=-\frac{4}{5}\epsilon l$ for longitudinal velocity increments proves that energy is transferred over scales with a positive constant flux ϵ [24]. Similarly, in incompressible magnetohydrodynamics (MHD) turbulence Yaglom's law on increments of the Elsasser variables (mixing the plasma velocity and the magnetic field) predicts $S(3,l)=-\frac{4}{3}\epsilon l$ [27]. We emphasize that these simple equations are derived from the general von Kármán–Howarth (vKH) equation only at the cost of additional assumptions of time stationarity, space homogeneity, and local (or full) isotropy. A recent derivation of the vKH equation for incompressible isotropic Hall MHD has been obtained in [28]. In data analyses, any rigorous demonstration of an energy cascade must rest upon the correspondence between these predicted exact relations and their experimental measurements. Nonzero values of $S(3,l)$ can then be interpreted as evidence of a turbulent cascade, and a negative (positive) sign of $S(3,l)$ as a direct (inverse) energy cascade [29,30]. Here we deal with mirror mode turbulence for which no vKH equation has been derived so far. The physics of the mirror turbulence is indeed more complex since compressibility, anisotropies, and kinetic effects are present [10]. Although some progress has been achieved recently in fluid formulation of the nonlinear dynamics of these modes [26], a fluidlike turbulence theory of mirror modes is still out of reach. Nevertheless, in spite of these theoretical limitations, we show below that $S(3,l)$ calculated for the magnetic field increments is useful for revealing additional information about the mirror mode turbulence. We note that the other Cluster plasma data (density, velocity, and pressure) are available only at low time resolution (4 s) which cannot allow investigation of the time scales considered here ($\tau<10$ s).

Comparison of the normalized skewnesses of the four times series shows that over two decades of scales $B_{\mathrm{PDF}}(t)$, $B_C(t)$ and $B_R(t)$ have almost zero skewness, suggesting the absence of energy transfers (Fig. 9). It is interesting to notice that, despite the fact that $B_C(t)$ has a high degree of coherence, no energy transfer is observed over about two decades of scale. Note, however, a sharp increase of the skewness at the scale $\tau\sim 0.1$, which is of the same order as the size of the coherent structure in $B_C(t)$, since asymmetry is expected to appear at this scale. This result can be used to differentiate between scaling laws generated by a turbulent cascade and those due to a single coherent structure as in the case of $B_C(t)$. On the other hand, $B_O(t)$ has a finite and negative skewness below the scale $\tau\sim 8$ s and tends to zero at the very small scales $\tau<0.2$ s, indicating the presence of finite energy transfers from large to small scales.

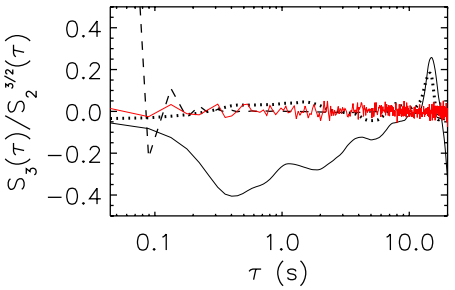

FIG. 9. (Color online) Normalized skewness of $B_O(t)$ (solid line), $B_R(t)$ (dotted line), $B_C(t)$ (dashed line), and $B_{\mathrm{PDF}}(t)$ (red line).

To further check the possibility of the existence of a constant energy flux over these scales, we calculate the compensated third-order SFs of signed increments: $S_O(3,\tau)/\tau^{2.2}$. As we can see, a relatively flat zone of scales that spans from $\tau\sim 0.2$ to ~ 3 s occurs (Fig. 10). Considering the theoretical limitations explained above, these observations can be interpreted only on the basis of analogies with hydrodynamics or MHD turbulence. Let us then assume that a vKH equation for mirror mode turbulence exists. If this equation reduces to a Yaglom-type equation [i.e., a linear relation between the energy flux ϵ and $S(3,l)$] under the assumptions of (space) time (homogeneity) stationarity, then one may view this zone as an inertial range of the mirror modes, for which the scaling $S_O(3,\tau)\sim-\epsilon\tau^{2.2}$ is a good approximation. The numerical values of ϵ can be inferred from Fig. 10 for possible comparisons with theories of mirror mode turbulence that still need to be built. The existence of a constant energy flux for the same range of scales evidenced in [10] is strong support for the proposed cascade scenario of the mirror modes. The increase of phase coherence in the same interval of scales suggests furthermore that these mirrors should be viewed as

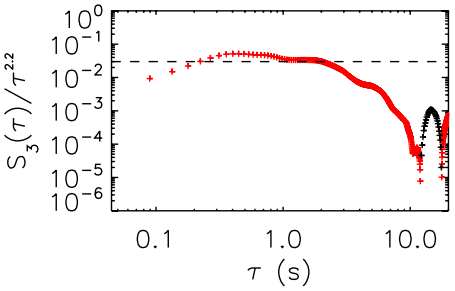

FIG. 10. (Color online) $S(3,\tau)$ calculated for signed increments: positive values (black) and negative values (red) compensated by $\tau^{2.2}$.

coherentlike structures rather than randomlike modes.

We notice that random phases do not necessarily imply absence of energy cascade. It is indeed well known that weak turbulence theories lead to energy cascades with predicted scaling even if random phases are generally assumed through the RPA [18,20]. Our results here concern the specific case of mirror structures, for which we prove that the structure of the phases is crucial. However, one could use the method presented in this work to test, in observations as well as in numerical simulations of weak turbulence, whether the energy cascades actually pass the test of phase randomization used here.

V. CONCLUSIONS

We have described a method to detect coherent structures in turbulent signals by using the technique of surrogate data sets and their SFs as discriminating statistics. We have introduced a general coherence index for estimating the degree of coherence as a function of scales, and have shown that its different orders ($q=1,3,4$) provide mainly the same information. We have shown that the second-order SFs can be used to quantify how accurately the surrogate data reproduce the power spectra, and to estimate the largest scale for which the SFs can be meaningfully calculated.

Using the PDFs of the increments of the observed and surrogate data, we have shown that the Fourier phases are responsible for creating the non-Gaussian tails of the PDFs, i.e., intermittency. The relationship between coherence and intermittency has been proved also by showing that the coherence index, estimated from the first-order SFs, can reproduce the information given by the flatness, usually used as the only measure of intermittency. This conclusion can be useful in situations where computation of high-order SFs is not possible (because, for instance, of limited stationarity or homogeneity) [4,31]. We have shown how one can use the technique to investigate asymmetries of the PDFs and prove the existence of energy transfers over a wide range of scales. When the method was applied to magnetosheath data, we have been able to bring strong evidence supporting the scenario of energy cascade of mirror structures previously suggested in [10].

We notice finally that many aspects have been studied (not shown in the present work) related to the choice of the windowing function, the conditioning (elimination of poor statistics) [32], the stability of the results for coherence with respect to randomization, and generation of other possible surrogates. All these technical aspects will be addressed in a separate presentation, including more applications to experimental data. Combination of multipoint data techniques such as the *k*-filtering method [33] to analyze power spectra and dispersion properties with the technique of surrogate data to study intermittency offers certainly a more complete and promising package to investigate space-plasma turbulence.

ACKNOWLEDGMENTS

I gratefully acknowledge Patrick Robert (FGM team) for providing the data used in this work. I thank M. Goldstein, G. Belmont, L. Rezeau, and A. Grandin for fruitful discussions. This work has been supported, in part, by the NASA Post Doctoral Program at the Goddard Space Flight Center.

[1] W. H. Matthaeus, M. L. Goldstein, and D. A. Roberts, J. Geophys. Res. **95**, 20673 (1990).
[2] M. L. Goldstein and D. A. Roberts, Phys. Plasmas **6**, 4154 (1999).
[3] C. P. Tu and E. Marsch, *MHD Structures, Waves and Turbulence in the Solar Wind: Observations and Theories* (Kluwer Academic, Belgium, 1997).
[4] T. Horbury and A. Balogh, Nonlinear Processes Geophys. **4**, 185 (1997).
[5] R. Bruno, V. Carbone, L. Sorriso-Valvo, and B. Bavassano, Geophys. Res. Lett. **108**, 1330 (2003).
[6] G. Belmont and L. Rezeau, J. Geophys. Res. **106**, 10751 (2001).
[7] O. Alexandrova, V. Carbone, P. Veltri, and L. Sorriso-Valvo, Astrophys. J. **674**, 1153 (2008).
[8] S. D. Bale, P. J. Kellogg, F. S. Mozer, T. S. Horbury, and H. Reme, Phys. Rev. Lett. **94**, 215002 (2005).
[9] D. Sundkvist, V. Krasnoselskikh, P. K. Shukla, A. Vaivads, M. Andre, S. Buchert, and H. Reme, Nature (London) **436**, 825 (2005).
[10] F. Sahraoui, G. Belmont, L. Rezeau, N. Cornilleau-Wehrlin, J. L. Pinçon, and A. Balogh, Phys. Rev. Lett. **96**, 075002 (2006).
[11] Y. Narita, K. Glassmeier, and R. A. Treumann., Phys. Rev. Lett. **97**, 191101 (2006).
[12] F. Levrier, E. Falgarone, and F. Viallefond, Astron. Astrophys. **456**, 205 (2006).
[13] J. Theiler, S. Eubank, A. Longtin, B. Galdrikian, and J. D. Farmer, Physica D **58**, 751 (1992).
[14] H. Kantz and T. Schreiber, *Nonlinear Time Series Analysis* (Cambridge University, Cambridge, U.K., 2004).
[15] T. Hada, D. Koga, and E. Yamamoto, Space Sci. Rev. **107**, 463 (2003).
[16] D. Koga and T. Hada, Space Sci. Rev. **107**, 495 (2003).
[17] D. Koga, A. C.-L. Chian, R. A. Miranda, and E. L. Rempel, Phys. Rev. E **75**, 046401 (2007).
[18] V. E. Zakharov, V. S. L'vov, and G. Falkovitch, *Kolmogorov Spectra of Turbulence I; Wave Turbulence* (Springer-Verlag, Berlin, 1992).
[19] F. Sahraoui, G. Belmont, and L. Rezeau, Phys. Plasmas **10**, 1325 (2003).
[20] Y. Choi, Y. V. Lvov, and S. Nazarenko, Physica D **201**, 121 (2005).
[21] J. Saur, H. Politano, A. Pouquet, and W. B. Matthaeus, Astron. Astrophys. **386**, 699 (2002).
[22] S. Galtier and A. Bhattacharjee, J. Plasma Phys. **10**, 3065 (2003).
[23] T. Schreiber and A. Schmitz, Physica D **142**, 346 (2000).

[24] U. Frisch, *Turbulence, the Legacy of A. N. Kolmogorov* (Cambridge University Press, Cambridge, U.K., 1996).
[25] F. Sahraoui, G. Belmont, J. L. Pinçon, L. Rezeau, A. Balogh, P. Robert, and N. Cornilleau-Wehrlin, Ann. Geophys. **22**, 2283 (2004).
[26] T. Passot and P. L. Sulem, J. Geophys. Res. **111**, A04203 (2006).
[27] H. Politano and A. Pouquet, Phys. Rev. E **57**, R21 (1998).
[28] S. Galtier, Phys. Rev. E **77**, 015302(R) (2008).
[29] E. Lindborg and J. Y. N. Choi, Phys. Rev. Lett. **85**, 5663 (2000).
[30] L. Sorriso-Valvo, R. Marino, V. Carbone, A. Noullez, F. Lepreti, F. L. P. Veltri, R. Bruno, B. Bavassano, and E. Pietropaolo, Phys. Rev. Lett. **99**, 115001 (2007).
[31] T. Dudok de Wit, Phys. Rev. E **70**, 055302(R) (2004).
[32] B. Hnat, S. C. Chapman, and G. Rowlands, J. Geophys. Res. **110**, A08206 (2005).
[33] F. Sahraoui, J. L. Pinçon, G. Belmont, L. Rezeau, N. Cornilleau-Wehrlin, P. Robert, L. Mellul, P. Canu, and G. Chanteur, J. Geophys. Res. **108**, 1335 (2003).